Kinetic Mechanism of the tRNA-Modifying Enzyme *S*-Adenosylmethionine:tRNA Ribosyltransferase-Isomerase (QueA)†

Steven G. Van Lanen and Dirk Iwata-Reuyl*

Department of Chemistry, Portland State University, Portland, Oregon 97207

Received February 4, 2003; Revised Manuscript Received March 13, 2003

ABSTRACT: The bacterial enzyme *S*-adenosylmethionine:tRNA ribosyltransferase-isomerase (QueA) catalyzes the unprecedented transfer and isomerization of the ribosyl moiety of *S*-adenosylmethionine (AdoMet) to a modified tRNA nucleoside in the biosynthesis of the hypermodified nucleoside queuosine. The complexity of this reaction makes it a compelling problem in fundamental mechanistic enzymology, and as part of our mechanistic studies of the QueA-catalyzed reaction, we report here the elucidation of the steady-state kinetic mechanism. Bi-substrate kinetic analysis gave initial velocity patterns indicating a sequential mechanism, and provided the following kinetic constants: $K_M^{tRNA} = 1.9 \pm 0.7$ μM and $K_M^{AdoMet} = 98 \pm 5.0$ μM. Dead-end inhibition studies with the substrate analogues *S*-adenosylhomocysteine and sinefungin gave competitive inhibition patterns against AdoMet and noncompetitive patterns against preQ$_1$-tRNA^{Tyr}, with K_i values of 133 ± 18 and 4.6 ± 0.5 μM for sinefungin and *S*-adenosylhomocysteine, respectively. Product inhibition by adenine was noncompetitive against both substrates under conditions with a subsaturating cosubstrate concentration and uncompetitive against preQ$_1$-tRNA^{Tyr} when AdoMet was saturating. Inhibition by the tRNA product (oQ-tRNA^{Tyr}) was competitive and noncompetitive against the substrates preQ$_1$-tRNA^{Tyr} and AdoMet, respectively. Inhibition by methionine was uncompetitive versus preQ$_1$-tRNA^{Tyr}, but noncompetitive against AdoMet. However, when methionine inhibition was investigated at high AdoMet concentrations, the pattern was uncompetitive. Taken together, the data are consistent with a fully ordered sequential bi-ter kinetic mechanism in which preQ$_1$-tRNA^{Tyr} binds first followed by AdoMet, with product release in the order adenine, methionine, and oQ-tRNA. The chemical mechanism that we previously proposed for the QueA-catalyzed reaction [Daoud Kinzie, S., Thern, B., and Iwata-Reuyl, D. (2000) *Org. Lett. 2,* 1307−1310] is consistent with the constraints imposed by the kinetic mechanism determined here, and we suggest that the magnitude of the inhibition constants for the dead-end inhibitors may provide insight into the catalytic strategy employed by the enzyme.

Extensive chemical modification of the constituent nucleosides is a hallmark of the post-transcriptional processing of tRNA (*1*), where nucleoside modification typically occurs at ~10% of the nucleosides in a particular tRNA, but can involve as many as 25% of the nucleosides (*1*). More than 80 modified nucleosides have been characterized (*1*), many of which are conserved across broad phylogenetic boundaries. The nature of nucleoside modification varies from simple methylation of the base or ribose ring to extensive hypermodification of the canonical bases, the latter of which can result in radical structural changes and involve multiple enzymatic steps to complete.

The enzyme *S*-adenosylmethionine:tRNA ribosyltransferase-isomerase (QueA)[1] catalyzes the unprecedented transfer and isomerization of the ribose moiety from *S*-adenosylmethionine (AdoMet) to 7-(aminomethyl)-7-deazaguanosine (preQ$_1$) modified tRNAs to give the hypermodified nucleoside epoxyqueuosine (oQ, Scheme 1), a remarkable reaction that includes the elimination of both methionine and adenine from AdoMet, and the rearrangement of the ribosyl moiety to form an epoxy carbocycle (*2*, *3*). QueA is part of an ensemble of enzymes that make up the biosynthetic pathway to the hypermodified nucleoside queuosine (Q, Scheme 2), the most radically modified nucleoside known to occur in tRNA. Queuosine and its derivatives are found exclusively at position 34 (the wobble position of the anticodon) of bacterial and eukaryotic tRNAs encoding the amino acids asparagine, aspartic acid, histidine, and tyrosine (*4*). Each of these tRNAs possesses the genetically encoded anticodon sequence GUN, where N can be any nucleotide. A definitive picture of the biochemical function or functions of queuosine has yet to emerge, but the presence or absence of queuosine-

† This work supported by a grant from the National Science Foundation (MCB-9733746).

* To whom correspondence should be addressed: Department of Chemistry, Portland State University, P.O. Box 751, Portland, OR 97207-0751. Phone: (503) 725-5737. Fax: (503) 725-9525. E-mail: iwatareuyld@pdx.edu.

[1] Abbreviations: Q, queuosine; oQ, epoxyqueuosine; AdoMet, *S*-adenosylmethionine; preQ$_1$, 7-(aminomethyl)-7-deazaguanine; TGT, tRNA-guanine transglycosylase; QueA, *S*-adenosylmethionine:tRNA ribosyltransferase-isomerase; MAT, *S*-adenosylmethionine synthetase; DTT, dithiothreitol; IPTG, isopropyl β-D-thiogalactopyranoside; glygly, glycylglycine; TCA, trichloroacetic acid; DEPC, diethylpyrocarbonate; HPLC, high-pressure liquid chromatography; SDS−PAGE, sodium dodecyl sulfate−polyacrylamide gel electrophoresis.

10.1021/bi034197u CCC: $25.00
Published on Web 04/18/2003

Scheme 1: QueA-Catalyzed Reaction

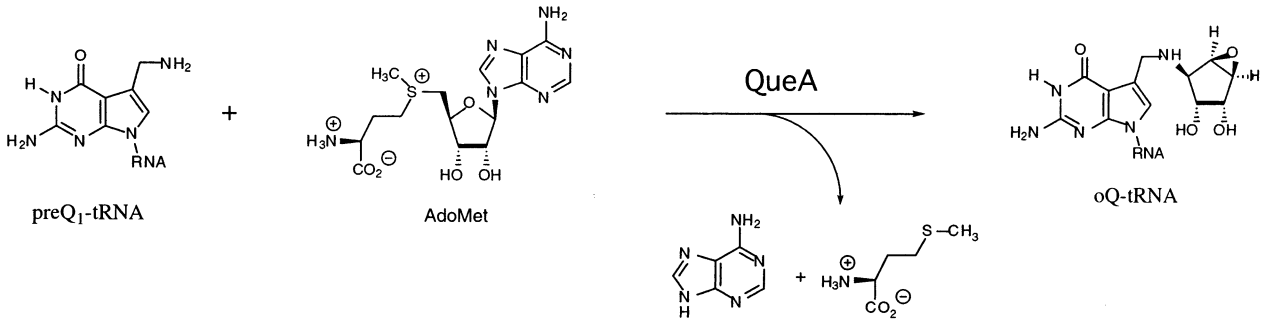

Scheme 2: *De Novo* Queuosine Biosynthetic Pathway in Bacteria

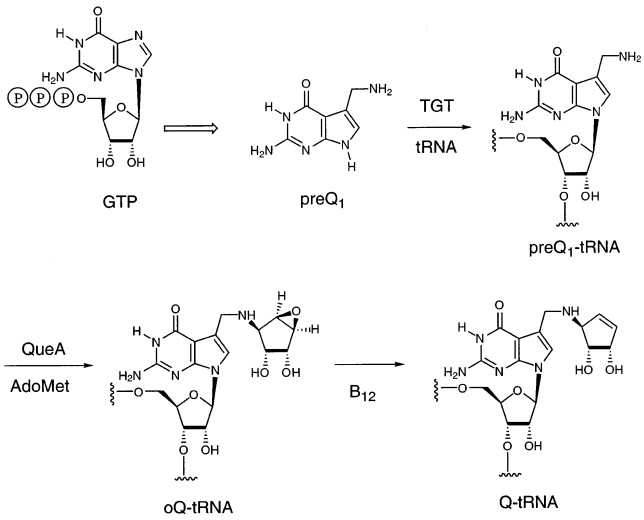

modified tRNA has been correlated with a variety of physiological phenomena, from eukaryotic cell development and proliferation (*5*−*8*) to translational frame shifts essential to retroviral protein biosynthesis (*9*−*11*) and the ability of pathogenic bacteria to invade and proliferate in human tissue (*12*, *13*). Underlying most of these phenomena is a potential role in modulating translational fidelity, consistent with the location of queuosine in the anticodon.

Although ubiquitous in both eukarya and bacteria, only bacteria are capable of *de novo* queuosine biosynthesis (Scheme 2). Eukaryotes utilize a salvage system and acquire queuosine as a nutrient factor and from intestinal flora (*14*), and insert queuine (the free base) directly into the appropriate tRNA with the enzyme tRNA-guanine transglycosylase (TGT) (*15*). A related TGT is part of the *de novo* biosynthesis in bacteria (*16*), but in this case, the substrate is the queuosine precursor $preQ_1$ (Figure 2), which appears to be derived from GTP (*17*). The correlation of bacterial pathogenicity with the presence of queuosine-modified tRNA (*12*, *13*) renders the queuosine pathway a potential target for antibacterials, and a recent report has described the development of inhibitors (*18*) for the bacterial TGT, the only other enzyme in the pathway identified to date.

The QueA-catalyzed reaction is the only known reaction in biology in which the ribosyl moiety of AdoMet is transferred to another chemical species, and the complexity of the reaction makes it a compelling problem in fundamental mechanistic enzymology (*3*, *19*). In previous work, we addressed the regiochemistry of C−N bond formation in the reaction using stable isotope experiments, and on the basis of the data proposed a chemical mechanism to account for the reaction (*19*). Having recently carried out a full characterization of the recombinant enzyme (*25*), we report here the first step in defining the kinetics of the enzyme-catalyzed reaction with the elucidation of the steady-state kinetic mechanism, determined through bi-substrate kinetic analysis, inhibition studies with two substrate analogues, and full product inhibition studies. The implications of the data for the previously proposed chemical mechanism and catalysis by the enzyme are discussed.

EXPERIMENTAL PROCEDURES

General. Buffers, salts, adenine, methionine, sinefungin, and *S*-adenosylhomocysteine (SAH), all of highest quality grade, were purchased from Sigma unless otherwise noted. Ampicillin, DTT, and IPTG were from U.S. Biologicals. [U-^{14}C]Glucose (46 mCi/mmol) was from ICN or Moravek. *Escherichia coli* tRNA tyrosine-specific I (HPLC standard) was from Sigma, and bulk *E. coli* MRE600 tRNA was from Roche. Glutathione Sepharose 4B was purchased from Amersham Biosciences. POROS chromatography resins were from PerSeptive Biosystems. Benzoylated-naphthoylated DEAE-cellulose (BND-cellulose), benzoylated DEAE-cellulose (BD-cellulose), and DEAE-cellulose were from Sigma, and NACS resin was from BRL Life Technologies, Inc. Whatman GF-B disks were from Fisher. Centriprep YM-30, Centricon YM-10, and Centricon YM-3 units were from Amicon. Dialysis was performed in Slide-A-Lyzer cassettes from Pierce. Buffers made for RNA work were prepared with DEPC-treated water and filtered through Cameo 25ES nitrocellulose filters from Osmonics, Inc. Protein concentrations were based on the Bradford dye binding procedure (Bio-Rad). Cytoscint ES liquid scintillation cocktail was from ICN.

Instrumentation. Centrifugation was performed with an Avanti J-20 XP centrifuge using JA-25.50 and JA-10 rotors, an LE-80K ultracentrifuge using a Ti-60 rotor, and a model TJ-6 swinging bucket centrifuge, all from Beckman Coulter, Inc. UV−vis spectrophotometry was performed with the Varian Cary 100 Bio spectrophotometer. HPLC was carried out with a Hitachi system consisting of the LACHROM software, the D-7000 System Manager, an L-7100 pump, and an L-4500A diode array detector. Temperatures were maintained for enzyme assays with a GeneAmp 2400 thermocycler from Perkin-Elmer. Sonication was carried out with a model W-375 sonicator from Heat Systems-Ultrasonics, Inc. Protein and nucleic acid PAGE was carried out with the Mini Protean III from Bio-Rad. Radioactivity from

enzyme assays was quantified with a Beckman LS 6500 liquid scintillation counter. A Molecular Dynamics Typhoon 9200 variable mode imager with ImageQuant 5.2 software was used to measure and analyze radioactivity in gels, and for fluorescence detection of ethidium bromide- or SybrGreen-stained nucleic acids in PAGE and agarose gels.

Bacterial Strains, Plasmids, and Enzymes. *E. coli* DH5α was from Gibco BRL Life Technologies, and *E. coli* BL21-(DE3) was from Stratagene. The *E. coli queA* deletion mutant K12QueA (*2*) and plasmid pGEX-QA (*2*) were generous gifts from H. Kersten (Universität Erlangen, Erlangen, Germany). 6-Phosphogluconate dehydrogenase type V from torula yeast was purchased from ICN as an ammonium sulfate suspension. L-Glutamic dehydrogenase type I from bovine liver, pyruvate kinase type II from rabbit muscle, glucose-6-phophate dehydrogenase type VII from baker's yeast, and myokinase from rabbit muscle were from Sigma, also as ammonium sulfate suspensions. Phosphoriboisomerase from torula yeast and hexokinase type F-300 from baker's yeast were from Sigma as lyophilized powders and were stored in 50% glycerol and the appropriate buffer at −90 °C. Recombinant adenine phosphoribosyltransferase (APRTase) was overproduced from pQEAPT1 in *E. coli* strain B25 (B25/pQEAPT1, a generous gift form M. Taylor, Indiana University, Bloomington, IN). Expression and purification of APRTase were essentially as described previously (*20*, *21*). The enzyme was judged to be ∼95% pure by SDS−PAGE analysis. Activity was measured as described previously (*22*). Recombinant *S*-adenosylmethionine synthetase (MAT) from *E. coli* was overproduced from pK8 (*23*) in *E. coli* DH5α (pK8, a generous gift of G. Markham, Fox Chase Cancer Center, Philadelphia, PA). Expression and streptomycin sulfate and ammonium sulfate purification steps were as described previously (*24*). The enzyme was enriched to ∼80% as judged by SDS−PAGE; activity was measured as described previously (*24*). Recombinant 5-phosphoribosyl-1-pyrophosphate (PRPP) synthetase from *Salmonella typhimurium* was overproduced from pBRS11R in *E. coli* DH5α (pBRS11R, a generous gift from V. L. Schramm, Albert Einstein College of Medicine, Bronx, NY). Overproduction of the recombinant GST−QueA conjugate was carried out as described previously (*25*). Synthesis and purification of [U-*ribosyl*-^{14}C]AdoMet and preQ$_1$-tRNA^{Tyr} were carried out as described previously (*25*).

Purification of oQ-tRNA^{Tyr} from E. coli MRE600. Fifty milligrams of crude *E. coli* MRE600 tRNA was dissolved in 50 mM sodium acetate (pH 5), 10 mM $MgCl_2$, and 0.4 M NaCl, and then loaded onto a column of BD cellulose (2.6 cm × 40 cm, ∼160 mL) equilibrated in the same buffer (buffer A). A linear gradient (1 L) was applied to 1.1 M NaCl, followed by an additional 0.3 L of buffer A with 1.1 M NaCl, and finally 0.3 L of buffer A containing 1.1 M NaCl and 9.5% (v/v) ethanol. The elution, monitored by A_{260}, was carried out at room temperature with a flow rate of approximately 1.5 mL/min. The oQ-tRNA^{Tyr} eluted during the application of the 1.1 M NaCl/9.5% ethanol mixture, and fractions containing oQ-tRNA^{Tyr} were pooled, concentrated using Centricon YM-10 units, and dialyzed against 3 mM citrate (pH 6.3). Tyrosine-specific tRNA comprised approximately 60% of the total A_{260} as judged from tyrosine-tRNA synthetase activity (*26*).

Enzyme Assays. QueA activity was measured by the incorporation of [U-*ribosyl*-^{14}C]AdoMet into tRNA as previously described (*25*). Assays were carried out in 100 mM glygly (pH 8.7), 100 mM KCl, 0.5 mM DTT, 100 mM EDTA, and 50 nM GST−QueA conjugate at 37 °C under initial velocity conditions as determined by time course assays. When low tRNA concentrations were present (≤50 μg), reactions were terminated by the initial addition of carrier tRNA to bring the total amount of tRNA to 50 μg, followed by the addition of 3 volumes of cold 10% TCA. The precipitated tRNA was collected on Whatmen GF-B filters by vacuum filtration, washed with cold 5% TCA followed by ethanol, and dried, and the radioactivity was quantified by liquid scintillation counting. For high tRNA concentrations (>50 μg), the reactions were terminated by decreasing the pH to 6.5 with the addition of acetic acid and heating at 95 °C for 5 min. The samples were loaded onto Quik-Sep columns containing 250 μL of DEAE-cellulose equilibrated in 50 mM imidazole (pH 6.5). The columns were washed with 15 volumes of 50 mM imidazole (pH 6.5), and the RNA was eluted with 7 column volumes of 50 mM imidazole (pH 6.5) and 1 M NaCl. The unreacted [U-*ribosyl*-^{14}C]AdoMet (wash) and RNA were separately collected, and the radioactivity was quantified by liquid scintillation counting. A minimum of four replicates were run.

Data Analysis. The kinetic nomenclature and methodology is that of Cleland (*27*−*29*). Data analysis was performed using KaleidaGraph software (Synergy Software, Reading, PA). Data were fit to the appropriate rate equation by using the nonlinear least-squares approach with the algorithms of Cleland (*30*). Mechanistic determinations were made by considering the standard error for each global fit, which in all cases was less than 10% for the best fit.

Bi-Substrate Kinetic Analysis. Enzyme reaction rates were determined as described above with variable [U-*ribosyl*-^{14}C]-AdoMet (10−400 μM) and preQ$_1$-tRNA^{Tyr} (0.38−7.5 μM) concentrations. Data were fit to the equations describing ping-pong (eq 1), sequential (eq 2), and rapid equilibrium random (eq 3) mechanisms:

$$v = \frac{V[A][B]}{K_b[A] + K_a[B] + [A][B]} \quad (1)$$

$$v = \frac{V[A][B]}{K_{ia}K_b + K_b[A] + K_a[B] + [A][B]} \quad (2)$$

$$v = \frac{V[A][B]}{\alpha K_a K_b + \alpha K_b[A] + \alpha K_a[B] + [A][B]} \quad (3)$$

where K_a and K_b are the Michaelis constants for the two substrates, K_{ia} is the dissociation constant for the enzyme−substrate A complex, α is the factor by which binding one substrate alters the others binding, and V is the maximal velocity. The dissociation constant for B was determined from the relationship $K_{ib} = K_{ia}(K_b/K_a)$.

Dead-End Inhibition. Enzyme reaction rates were determined as described above in the presence of the substrate analogues SAH (0−50 μM) and sinefungin (0−100 μM). Kinetic data were acquired with preQ$_1$-tRNA^{Tyr} as the variable substrate (0.18−3.75 μM) and subsaturating and

saturating [U-*ribosyl*-^{14}C]AdoMet concentrations (25 and 1000 μM, respectively), and with [U-*ribosyl*-^{14}C]AdoMet as the variable substrate (10−400 μM) and a subsaturating preQ$_1$-tRNA^{Tyr} concentration (0.75 μM). All data sets were initially fit to the simple equations for competitive (eq 4), uncompetitive (eq 5), and noncompetitive inhibition (eq 6)

$$v = \frac{VS}{K_m(1 + I/K_{is}) + S} \quad (4)$$

$$v = \frac{VS}{K_m + S(1 + I/K_{ii})} \quad (5)$$

$$v = \frac{VS}{K_m(1 + I/K_{is}) + S(1 + I/K_{ii})} \quad (6)$$

where S is the varied substrate concentration, I is the inhibitor concentration, K_{is} is the inhibition constant from the slope term, and K_{ii} is the inhibition constant for the intercept term. After preliminary mechanistic evaluations were made from best fits to the above equations, the data were fit to the appropriate full equations for an ordered sequential mechanism. With AdoMet as the variable substrate, the inhibition data were best fit to the equation for competitive inhibition (eq 7), while with tRNA as the variable substrate, the data were best fit to the equation for uncompetitive inhibition with tRNA binding first (eq 8). The parameters are defined as described above.

$$v = \frac{VB}{K_b(1 + I/K_i + K_{ia}/A) + B(1 + K_a/A)} \quad (7)$$

$$v = \frac{VA}{K_a + K_{ia}K_b/B + A(1 + K_b/B + K_bI/K_iB)} \quad (8)$$

Product Inhibition. Enzyme reaction rates were determined as described above in the presence of the products adenine, methionine, and oQ-tRNA^{Tyr}. Inhibitor concentrations were varied with preQ$_1$-tRNA^{Tyr} (0.75 μM) versus [U-*ribosyl*-^{14}C]-AdoMet (10−200 μM) as follows: adenine (from 0 to 360 μM), methionine (from 0 to 360 μM), and oQ-tRNA^{Tyr} (from 0 to 50 μM). Inhibitor concentrations were varied with [U-*ribosyl*-^{14}C]AdoMet (50 μM) versus preQ$_1$-tRNA (0.38−7.5 μM) as follows: adenine (from 0 to 342 μM), methionine (from 0 to 342 μM), and oQ-tRNA^{Tyr} (from 0 to 20 μM). Inhibition by adenine and methionine was also investigated at high substrate concentrations; with a constant [U-*ribosyl*-^{14}C]AdoMet concentration (500 μM), inhibition by adenine (0−100 μM) was investigated with variable preQ$_1$-tRNA^{Tyr} (15−33 μM), and with a constant preQ$_1$-tRNA^{Tyr} concentration (10 μM), inhibition by methionine (0−360 μM) was investigated with variable [U-*ribosyl*-^{14}C]AdoMet (500−2000 μM). As with substrate analogue inhibition, the product inhibition data were initially fit to the simple inhibition equations (eqs 4−6), followed by fitting to the appropriate full equations.

With preQ$_1$-tRNA^{Tyr} as the variable substrate and subsaturating AdoMet, and the presence of product inhibitor, data were fit to the equations for noncompetitive inhibition with adenine (eq 9), uncompetitive inhibition with methionine (eq 10), and competitive inhibition with oQ-tRNA (eq 11)

$$v = \frac{VA}{K_a(1 + K_bK_{ia}/K_aB)(1 + I/K_{is}) + A(1 + K_b/B)(1 + I/K_{ii})} \quad (9)$$

$$v = \frac{VA}{K_a(1 + K_bK_{ia}/K_aB) + A(1 + K_b/B)(1 + I/K_{ii})} \quad (10)$$

$$v = \frac{VA}{K_a(1 + K_bK_{ia}/K_aB)(1 + I/K_{is}) + A(1 + K_b/B)} \quad (11)$$

where the parameters are defined as described above. With AdoMet as the variable substrate and subsaturating preQ$_1$-tRNA^{Tyr}, the inhibition data for adenine, methionine, and oQ-tRNA were fit to the equation for noncompetitive inhibition against the second substrate (eq 12).

$$v = \frac{VB}{K_b(1 + K_{ia}/A)(1 + I/K_{is}) + B(1 + K_a/A)(1 + I/K_{ii})} \quad (12)$$

RESULTS

Enzyme and Substrate Preparation. Previous experiments (*25*) demonstrated that the presence of the GST domain in the GST−QueA fusion protein had no effect on the activity of QueA, so all experiments were carried out utilizing the GST−QueA conjugate. Purification was essentially as described previously (*25*), and provided protein that was homogeneous by SDS−PAGE.

The preparation of [U-*ribosyl*-^{14}C]AdoMet was accomplished as described previously (*25*) using the methodology of Schramm and co-workers for the initial synthesis of [U-*ribosyl*-^{14}C]ATP (*31*), followed by the MAT-catalyzed conversion of [U-*ribosyl*-^{14}C]ATP to AdoMet according to Park et al. (*32*). AdoMet with specific activity and purity was then obtained after reverse-phase HPLC purification. PreQ$_1$-tRNA^{Tyr} was overproduced from K12QueA/pTrc-Tyr and purified as previously described (*25*).

Epoxyqueuosine-containing tRNA^{Tyr} (oQ-tRNA^{Tyr}) was purified from bulk *E. coli* MRE600 tRNA by a modification of the procedure described for preQ$_1$-tRNA^{Tyr} (*25*). The

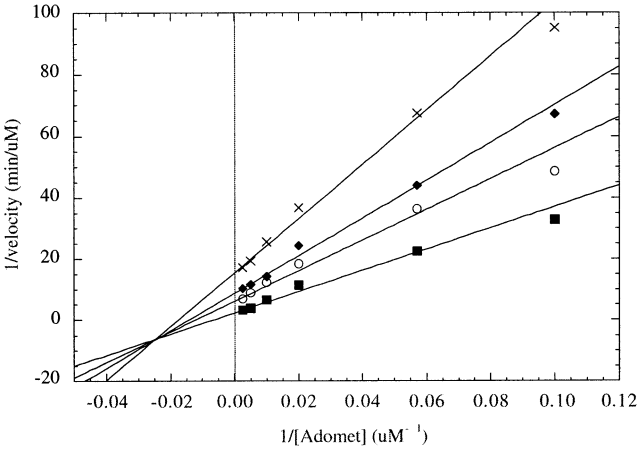

FIGURE 1: Bi-substrate kinetic analysis. Reaction assays were carried out as described in Experimental Procedures. Initial velocity plots with variable AdoMet at multiple fixed concentrations of preQ$_1$-tRNA^{Tyr}. PreQ$_1$-tRNA^{Tyr} concentrations were (×) 0.38, (◆) 0.75, (○) 1.5, and (■) 7.5 μM. Data were fit to eq 2.

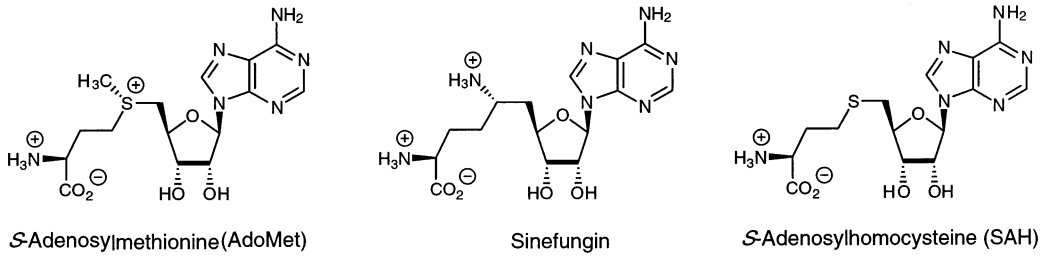

FIGURE 2: Chemical structures of AdoMet, sinefungin, and SAH.

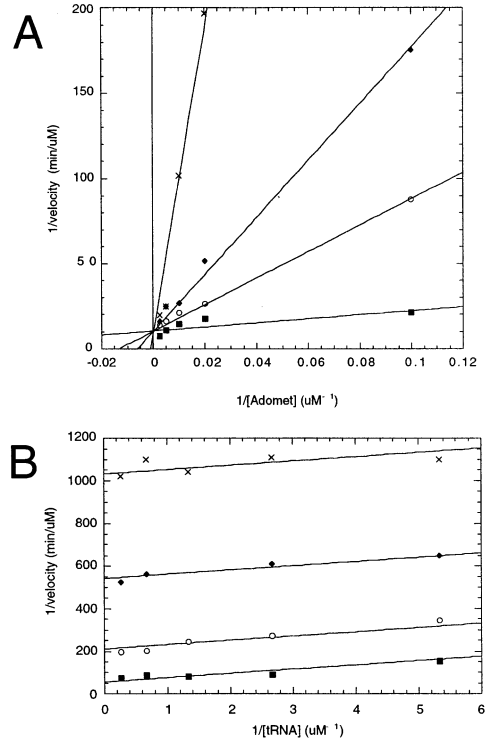

FIGURE 3: Inhibition by *S*-adenosylhomocysteine. (A) Inhibition with variable AdoMet. The concentrations of SAH were (■) 0, (○) 5, (◆) 10, and (×) 50 μM. Data were fit to eq 7. (B) Inhibition with variable preQ$_1$-tRNA^{Tyr}. The concentrations of SAH were (■) 0, (○) 5, (◆) 30, and (×) 100 μM. Data were fit to eq 8.

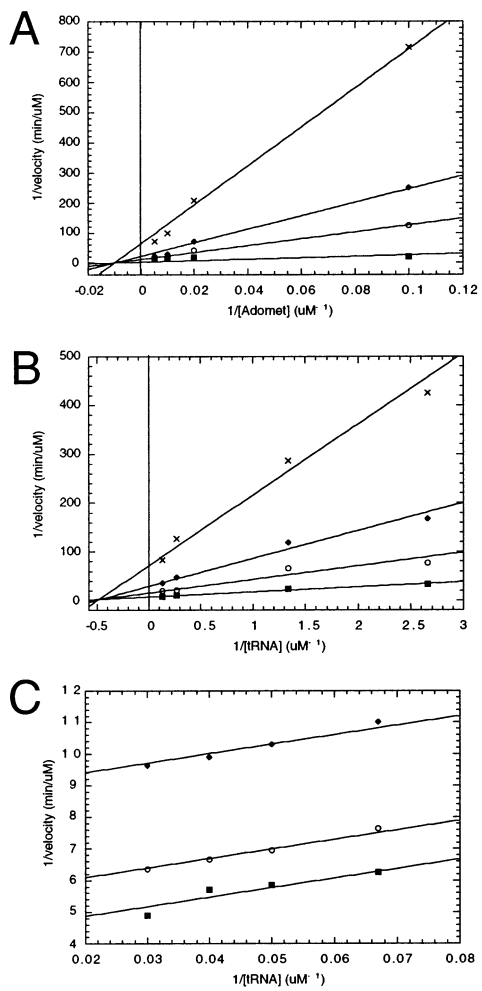

FIGURE 4: Product inhibition with adenine. (A) Adenine inhibition with variable AdoMet. The concentrations of adenine were (■) 0, (○) 20, (◆) 100, and (×) 360 μM. The concentration of preQ$_1$-tRNA^{Tyr} was 0.75 μM. Data were fit to eq 12. (B) Adenine inhibition with variable preQ$_1$-tRNA^{Tyr} when AdoMet is subsaturating (50 μM). The concentrations of adenine were (■) 0, (○) 20, (◆) 100, and (×) 342 μM. Data were fit to eq 9. (C) Adenine inhibition with variable preQ$_1$-tRNA^{Tyr} when AdoMet is saturating (1 mM). The concentrations of adenine were (■) 0, (○) 20, and (◆) 100 μM. Data were fit to eq 10.

MRE600 strain of *E. coli* has been shown to contain predominantly epoxyqueuosine in the relevant tRNAs instead of queuosine (*33*), a result of decreased cobalamin metabolism when grown under typical commercial conditions (*34*). Purification was carried out by chromatography on BD-cellulose, which provided tRNA highly enriched in oQ-tRNA^{Tyr} (~60% corresponded to oQ-tRNA^{Tyr}).

Bi-Substrate Kinetic Analysis. Bi-substrate initial velocity patterns were analyzed to deduce between sequential or ping-pong mechanisms. When the concentration of AdoMet was varied with constant preQ$_1$-tRNA^{Tyr} (or variable preQ$_1$-tRNA^{Tyr} at a constant AdoMet concentration, data not shown), reciprocal plots gave an intersecting pattern that crossed to the left of the vertical axis and below the horizontal axis as seen in Figure 1. The data clearly indicate a requirement for binding of both substrates for formation of a ternary complex before catalysis can occur, thus ruling out a ping-pong mechanism. Kinetic constants derived from fitting the data to eq 2 are essentially identical to the results from single-substrate kinetics as determined previously (*25*), with a K_M^{tRNA} of 1.9 ± 0.7 μM and a K_M^{AdoMet} of 98 ± 5.0 μM. The dissociation constant for preQ$_1$-tRNA^{Tyr} (K_{ia}) was 1.0 ± 0.3 μM, slightly lower than the K_M as expected from the initial velocity patterns.

Dead-End Inhibition. Substrate analogue inhibition was used to differentiate between ordered and random sequential mechanisms. These were performed using *S*-adenosylhomocysteine (SAH) and sinefungin, both structural analogues of AdoMet (Figure 2). SAH and sinefungin (data not shown for sinefungin) exhibited competitive inhibition with respect

Table 1: Bi-Substrate Kinetic Analysis and Substrate Analogue Inhibition

substrate	inhibitor	inhibition pattern[a]	K_m[b] (μM)	K_i[c] (μM)	K_{ia}[b] (μM)
AdoMet	–	–	98 ± 5.0	–	52 ± 6.0
	SAH	C		4.6 ± 0.5	
	sinefungin	C		133 ± 18	
preQ$_1$-tRNA^{Tyr}	–	–	1.9 ± 0.7	–	1.0 ± 0.3
	SAH	UC		0.80 ± 0.03	
	singefungin	UC		5.5 ± 0.1	

[a] C represents competitive inhibition and UC uncompetitive inhibition. [b] Values for the kinetic constants were obtained from fitting the data to eq 2 for an ordered sequential mechanism. [c] Values for the kinetic constants were obtained from data fits to eq 7 for competitive inhibition against AdoMet and eq 8 for uncompetitive inhibition against preQ$_1$-tRNA^{Tyr}.

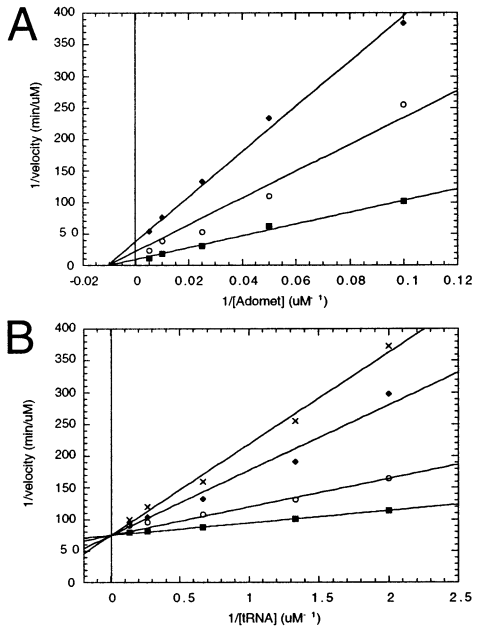

FIGURE 5: Product inhibition with oQ-tRNA. (A) oQ-tRNA^{Tyr} inhibition vs AdoMet. Fixed concentrations of oQ-tRNA were (■) 0, (○) 100, and (◆) 250 μM. The preQ$_1$-tRNA^{Tyr} concentration was 1.5 μM. Data were fit to eq 12. (B) oQ-tRNA^{Tyr} inhibition vs preQ$_1$-tRNA^{Tyr}. Fixed concentrations of oQ-tRNA^{Tyr} were (■) 0, (○) 5, (◆) 10, and (×) 20 μM. The AdoMet concentration was 25 μM. Data were fit to eq 11.

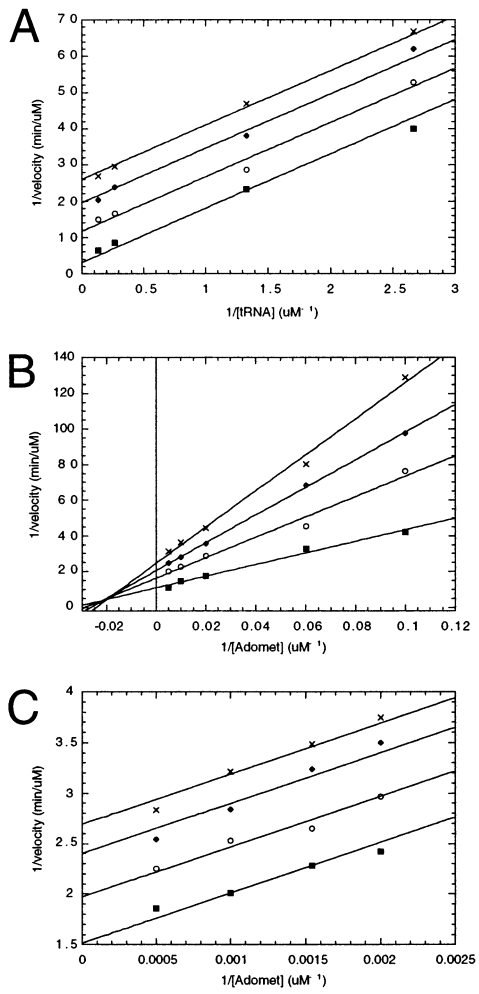

FIGURE 6: Product inhibition with methionine. (A) Methionine inhibition vs preQ$_1$-tRNA^{Tyr}. Fixed concentrations of methionine were (■) 0, (○) 20, (◆) 100, and (×) 342 μM. The AdoMet concentration was 50 μM. Data were fit to eq 10. (B) Methionine inhibition vs AdoMet. Fixed concentrations of methionine were (■) 0, (○) 20, (◆) 100, and (×) 360 μM. The preQ$_1$-tRNA^{Tyr} concentration was 0.75 μM. Data were fit to eq 12. (C) Methionine inhibition vs AdoMet at high AdoMet concentrations. Fixed concentrations of methionine were (■) 0, (○) 20, (◆) 100, and (×) 360 μM. The preQ$_1$-tRNA^{Tyr} concentration was 10 μM. Data were fit to eq 10.

to AdoMet (Figure 3A), consistent with ordered binding. The two inhibitors displayed uncompetitive inhibition with respect to preQ$_1$-tRNA^{Tyr} (Figure 3B), consistent with ordered binding in which preQ$_1$-tRNA^{Tyr} binds first followed by AdoMet to form the ternary complex. Fitting the inhibition data versus AdoMet to the full equation for competitive inhibition in an ordered sequential mechanism (eq 7) yielded K_i values of 133 ± 18 and 4.6 ± 0.5 μM for sinefungin and SAH, respectively. All kinetic parameters are listed in Table 1.

Product Inhibition. Product inhibition studies with adenine, methionine, and oQ-tRNA^{Tyr} were undertaken to provide further evidence to support substrate binding order, and to elucidate the order of product release. Inhibition by adenine was noncompetitive versus both substrates (Figure 4A,B) at unsaturating cosubstrate concentrations, indicating binding to a distinct enzyme form separated by reversible steps, consistent with an ordered addition of substrates and release of adenine first. When adenine inhibition was examined under conditions of saturating AdoMet, adenine exhibited uncompetitive inhibition versus preQ$_1$-tRNA^{Tyr} (Figure 4C). These patterns are consistent with ordered substrate binding in which preQ$_1$-tRNA^{Tyr} binds first and adenine is released first.

oQ-tRNA^{Tyr} displayed competitive inhibition against preQ$_1$-tRNA^{Tyr} (Figure 5B), consistent with an ordered mechanism in which preQ$_1$-tRNA^{Tyr} and oQ-tRNA^{Tyr} bind to the free form of the enzyme, binding first and dissociating last,

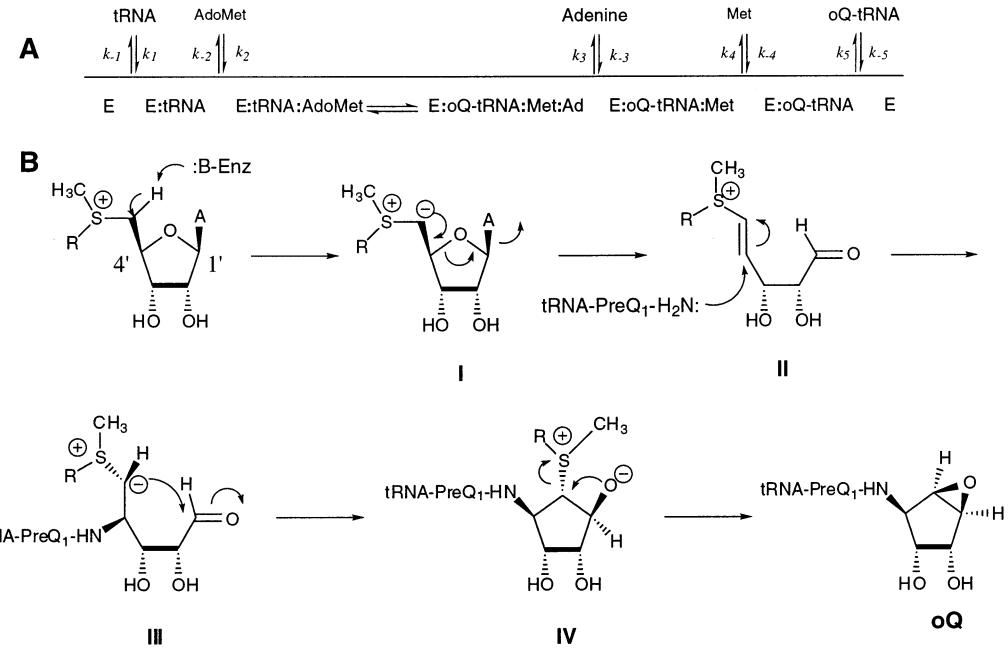

FIGURE 7: Proposed kinetic (A) and chemical (B) mechanisms for the QueA-catalyzed reaction.

Table 2: Product Inhibition Patterns and Kinetic Constants

inhibitor	varied substrate	[cosubstrate] (μM)[a]	inhibition pattern[b]	K_{is} (μM)[c]	K_{ii} (μM)[c]
adenine	preQ$_1$-tRNA^{Tyr}	50	NC	11.2 ± 2.0	21.0 ± 4.0
	preQ$_1$-tRNA^{Tyr}	1000	UC		21.1 ± 0.2
	AdoMet	0.65	NC	12.2 ± 1.7	46.1 ± 5.5
methionine	preQ$_1$-tRNA^{Tyr}	50	UC		62.8 ± 6.1[d]
	AdoMet	0.65	NC	21.9 ± 1.8[e]	8.9 ± 1.7
	AdoMet (high)	10	UC		15.3 ± 2.0
oQ-tRNA^{Tyr}	preQ$_1$-tRNA^{Tyr}	25	C	2.3 ± 0.4	
	AdoMet	1.3	NC	10.2 ± 0.6	12.5 ± 0.2

[a] All experiments were carried out with unsaturating cosubstrate except adenine inhibition against preQ$_1$-tRNA^{Tyr} (1 mM AdoMet) and methionine inhibition against AdoMet (10 μM preQ$_1$-tRNA^{Tyr}). [b] NC represents noncompetitive, UC uncompetitive, and C competitive. [c] Kinetic constants were calculated from fits to eqs 9−12 as discussed in the text. Equations describing K_{ii} and K_{is} in terms of kinetic constants have been described elsewhere (*44*). [d] When methionine can act as both a product and dead-end inhibitor (binding to the E−tRNA complex), the expression for the intercept inhibition constant is $K_{ii} = (K_{ib}K_pK_{iq}K_{ir}/K_bK_rK_{ip})(1 + K_b/B)/(1 + K_{ib}K_{ir}K_pK_{iq}/K_rK_{ip}K_iB)$, where K_i is the constant for dissociation of methionine from the dead-end complex. [e] The expression for the slope inhibition constant is $K_{is} = K_i(1 + K_{ia}/A)$, where K_i is defined as described above.

respectively. When preQ$_1$-tRNA^{Tyr} was held constant, oQ-tRNA^{Tyr} showed noncompetitive inhibition against AdoMet (Figure 5A) as expected for an ordered mechanism.

The inhibition observed by methionine was initially perplexing in that it exhibited an uncompetitive pattern against preQ$_1$-tRNA^{Tyr} (Figure 6A) and noncompetitive inhibition against AdoMet (Figure 6B). Uncompetitive inhibition against both substrates is expected for an ordered mechanism in which methionine is released second as suggested from the results of the above experiments. However, when methionine inhibition was examined at high AdoMet concentrations (or a low methionine concentration, data not shown), uncompetitive inhibition was observed (Figure 6C).

Collectively, the data support a completely ordered sequential bi-ter kinetic mechanism, with binding of preQ$_1$-tRNA^{Tyr} followed by AdoMet to form the ternary complex. Products are then released in the following order: adenine, methionine, and oQ-tRNA^{Tyr} (Figure 7A). All of the relevant kinetic parameters and inhibition patterns are summarized in Table 2.

DISCUSSION

A minimal kinetic mechanism for the QueA-catalyzed reaction consistent with the kinetic data reported above is an ordered sequential bi-ter mechanism as shown in Figure 7A, with binding of preQ$_1$-tRNA^{Tyr} followed by AdoMet to form a ternary complex, followed by reaction and product release in the following order: adenine, methionine, and oQ-tRNA^{Tyr}. Initial velocity studies clearly indicate that all substrates must be present before product is released, and because both SAH and sinefungin behave as competitive inhibitors against AdoMet, a random sequential mechanism can be eliminated; competitive inhibition versus AdoMet is only consistent with ordered binding. Furthermore, both inhibitors exhibited an uncompetitive pattern versus preQ$_1$-tRNA^{Tyr}, consistent with binding of preQ$_1$-tRNA^{Tyr} followed by AdoMet. Noncompetitive inhibition would be observed if AdoMet were the first substrate to bind.

The data from product inhibition studies, in addition to further supporting our conclusions about substrate binding order, establish that product release is also ordered. With the exception of methionine inhibition, the initial velocity

data from product inhibition studies exhibited patterns consistent with ordered product release, with adenine released first and oQ-tRNA^{Tyr} last. The inhibition pattern exhibited by methionine, which is uncompetitive against preQ$_1$-tRNA^{Tyr} and noncompetitive against AdoMet (Figure 6A,B), is not expected for an ordered release with methionine leaving second; uncompetitive inhibition should be observed with both substrates. However, a noncompetitive pattern would be observed if dead-end inhibition were also occurring due to methionine binding to the enzyme•preQ$_1$-tRNA^{Tyr} complex (*35*). Given the strong binding observed for SAH, this seemed to be a plausible scenario, and was verified by examining inhibition at high AdoMet concentrations (or a low methionine concentration), conditions that force methionine and AdoMet to bind to different enzyme forms. Under these conditions, uncompetitive inhibition was observed (Figure 6C) as expected for ordered release of the second product.

Besides helping to clarify the kinetic mechanism, the kinetic behavior of the dead-end inhibitors SAH and sinefungin may offer insight into the chemistry of QueA catalysis. Sinefungin is both isosteric and isoelectronic with AdoMet, and not surprisingly binds to QueA with comparable affinity (assuming that $K_M \approx K_D$ for AdoMet). In contrast, SAH lacks both the substituent and associated positive charge of AdoMet and sinefungin, yet binds more than 20-fold more tightly to QueA than either of these compounds. Such behavior is consistent with binding of the sulfonium group of AdoMet in a hydrophobic environment. In the conversion of AdoMet to oQ, deprotonation of AdoMet at C5′ must occur at some point in the chemical mechanism (see Figure 7B). We previously proposed (*19*) that the acidity of the 5′-methylene hydrogens of AdoMet [p$K_a \sim 23$ (*36*)] revealed a chemical imperative for the unique utilization of AdoMet as a ribosyl donor; the ability to deprotonate at C5′ makes possible the key carbon−carbon bond construction between C5′ and C1′ of the ribosyl moiety. However, while a pK_a of ∼23 is in the range of values for other biochemically important carbon acids, the pK_a must be decreased significantly further for turnover to occur on a biologically useful time scale. The mechanism of enzymatic pK_a reduction in carbon acids has been investigated most thoroughly for α-carbonyl compounds, where it has been proposed that H-bonding from the enzyme to the carbonyl oxygen (*37*, *38*) is responsible for the pK_a reduction at the adjacent carbon. While this proposal is not universally embraced (*39*, *40*), the mechanism is clearly unavailable to sulfonium species, and in this case, pK_a reduction may instead be achieved in part by binding the sulfonium group in a hydrophobic environment, which would result in preferential stabilization of the transition state leading to the neutral ylide over the positively charged sulfonium. Such a phenomenon is proposed by Jordan et al. to be responsible in yeast pyruvate decarboxylase for the reduction of the pK_a at C2 and C2α of thiamin and the thiamin adduct, respectively (*41*). Here, a reduction in the pK_a at C2α of >9 units was observed upon binding to the enzyme, a change that correlated exactly to the reduced dielectric constant of the enzyme active site relative to water.

On the basis of the results of isotope tracer experiments, stereochemical considerations of the conversion of AdoMet to oQ, and chemical precedent (*36*, *42*, *43*), we proposed the mechanism outlined in Figure 7B to account for the chemical steps involved in the reaction (*19*). In this proposal, the first step is enzyme-catalyzed deprotonation of AdoMet at C5′ which generates the sulfonium ylide **I**, which can collapse to the vinyl sulfonium **II** by opening of the ribose ring with concomitant elimination of adenine. Although not shown explicitly, cleavage of the glycosidic C−N bond and release of adenine would only be expected to occur in concert with protonation of adenine (at either N7 or N3). Nucleophilic attack of the preQ$_1$ amine at the *re* face of C4′ then generates the new sulfonium ylide **III**, which can subsequently attack the *re* face of the C1′ (C3″ in oQ numbering) aldehyde to give the alkoxy carbocycle **IV**. Intramolecular S_N2 attack of the alkoxy oxygen on the adjacent carbon and elimination of methionine then give oQ.

In the proposed chemical mechanism, adenine is the first product formed, followed by the simultaneous formation of methionine and oQ. Although one cannot infer the timing of bond breaking and forming events from the order of product release as deduced from steady-state measurements, the proposed chemical mechanism for the QueA-catalyzed reaction (Figure 7) is consistent with the kinetic analysis reported here, and remains consistent if product release (i.e., adenine) precedes completion of all bond breaking and forming steps. Importantly, knowledge of the steady-state kinetic mechanism will now allow specific mechanistic questions to be formulated, the answers to which can be pursued through more detailed kinetic and chemical studies of the enzyme.

REFERENCES

1. Bjork, G. R. (1995) in *tRNA: Structure, Biosynthesis, and Function* (Soll, D., and RajBhandary, U. L., Eds.) pp 165−206, ASM Press, Washington, DC.
2. Slany, R. K., Bosl, M., Crain, P. F., and Kersten, H. (1993) *Biochemistry 32*, 7811−7817.
3. Slany, R. K., Bosl, M., and Kersten, H. (1994) *Biochimie 76*, 389−393.
4. Kersten, H. (1988) *BioFactors 1*, 27−29.
5. Kersten, H., and Kersten, W. (1990) in *Chromatography and Modification of Nucleosides Part B* (Gehrke, C. W., and Kuo, K. C. T., Eds.) pp B69−B108, Elsevier, Amsterdam.
6. Okada, N., Shindo-Okada, N., Sato, S., Itoh, Y. H., Oda, K., and Nishimura, S. (1978) *Proc. Natl. Acad. Sci. U.S.A. 75*, 4247−4251.
7. Owenby, R. K., Stulberg, M. B., and Jacobson, K. B. (1979) *Mech. Ageing Dev. 11*, 91−103.
8. White, B. N., Tener, G. M., Holden, J., and Suzuki, D. T. (1973) *J. Mol. Biol. 74*, 635−651.
9. Carlson, B. A., Kwon, S. Y., Chamorro, M., Oroszlan, S., Hatfield, D. L., and Lee, B. J. (1999) *Virology 255*, 2−8.
10. Jacks, T., Madhani, H. D., Masiarz, F. R., and Varmus, H. F. (1988) *Cell 55*, 447−458.
11. Hatfield, D., Feng, Y.-X., Lee, B. J., Rein, A., Levin, J. G., and Oroszlan, S. (1989) *Virology 173*, 736−742.
12. Durand, J., Okada, N., Tobe, T., Watarai, M., Fukuda, I., Suzuki, T., Nakata, N., Komatsu, K., Yoshikawa, M., and Sasakawa, C. (1994) *J. Bacteriol. 176*, 4627−4634.
13. Durand, J. M., Dagberg, B., Uhlin, B. E., and Bjork, G. R. (2000) *Mol. Microbiol. 35*, 924−935.
14. Kirtland, G. M., Morris, T. D., Moore, P. H., O'Brian, J. J., Edmonds, C. G., McCloskey, J. A., and Katze, J. R. (1988) *J. Bacteriol. 170*, 5633−5641.
15. Shindo-Okada, N., Okada, N., Ohgi, T., Goto, T., and Nishimura, S. (1980) *Biochemistry 19*, 395−400.
16. Okada, N., Noguchi, S., Kasai, H., Shindo-Okada, N., Ohgi, T., Goto, T., and Nishimura, S. (1979) *J. Biol. Chem. 254*, 3067−3073.
17. Kuchino, Y., Kasai, H., Nihei, K., and Nishimura, S. (1976) *Nucleic Acids Res. 3*, 393−398.

18. Gradler, U., Gerber, H. D., Goodenough-Lashua, D. M., Garcia, G. A., Ficner, R., Reuter, K., Stubbs, M. T., and Klebe, G. (2001) *J. Mol. Biol. 306* (18), 455−467.
19. Kinzie, S. D., Thern, B., and Iwata-Reuyl, D. (2000) *Org. Lett. 2*, 1307−1310.
20. Alfonzo, J. D., Crother, T. R., Guetsova, M. L., Daignan-Fornier, B., and Taylor, M. W. (1999) *J. Bacteriol. 181*, 347−352.
21. Alfonzo, J. D., Sahota, A., and Taylor, M. W. (1997) *Biochim. Biophys. Acta 1341*, 173−182.
22. Hochstadt, J. (1978) *Methods Enzymol. 51*, 558−567.
23. Boyle, S. M., Markham, G. D., Hafner, E. W., Wright, J. M., Tabor, H., and Tabor, C. W. (1984) *Gene 30*, 129−136.
24. Markham, G. D., Hafner, E. W., Tabor, C. W., and Tabor, H. (1980) *J. Biol. Chem. 255*, 9082−9092.
25. Van Lanen, S. G., Daoud Kinzie, S., Matthieu, S., Link, T., Culp, J., and Iwata-Reuyl, D. (2003) *J. Biol. Chem. 278*, 10491−10499.
26. Nishimura, S., Harada, F., Narushima, U., and Seno, T. (1967) *Biochim. Biophys. Acta 142*, 133−148.
27. Cleland, W. W. (1963) *Biochim. Biophys. Acta 67*, 188−196.
28. Cleland, W. W. (1963) *Biochim. Biophys. Acta 67*, 104−137.
29. Cleland, W. W. (1963) *Biochim. Biophys. Acta 67*, 173−187.
30. Cleland, W. W. (1977) *Adv. Enzymol. Relat. Areas Mol. Biol. 45*, 273−387.
31. Parkin, D. W., Leung, H. B., and Schramm, V. L. (1984) *J. Biol. Chem. 259*, 9411−9417.
32. Park, J., Tai, J., Roessner, C. A., and Scott, A. I. (1996) *Bioorg. Med. Chem. 4*, 2179−2185.
33. Phillipson, D. W., Edmonds, C. G., Crain, P. F., Smith, D. L., Davis, D. R., and McCloskey, J. A. (1987) *J. Biol. Chem. 262*, 3462−3471.
34. Frey, B., McCloskey, J. A., Kersten, W., and Kersten, H. (1988) *J. Bacteriol. 170*, 2078−2082.
35. Segel, I. (1975) *Enzyme Kinetics: Behavior and Analysis of Rapid Equilibrium and Steady-State Enzyme Systems*, John Wiley & Sons, New York.
36. Fava, A. (1985) in *Organic Sulfur Chemistry: Theoretical and Experimental Advances* (Bernardi, F., Csizmadia, I. G., and Mangini, A., Eds.) pp 299−354, Elsevier, Amsterdam.
37. Gerlt, J. A., Kozarich, J. W., Kenyon, G. L., and Gassman, P. G. (1991) *J. Am. Chem. Soc. 113*, 9667−9669.
38. Gerlt, J. A., and Gassman, P. G. (1993) *J. Am. Chem. Soc. 115*, 11552−11568.
39. Warshel, A. (1998) *J. Biol. Chem. 273*, 27035−27038.
40. Guthrie, J. P., and Kluger, R. (1993) *J. Am. Chem. Soc. 115*, 11569−11572.
41. Jordan, F., Li, H., and Brown, A. (1999) *Biochemistry 38*, 6369−6373.
42. Trost, B. M., and Melvin, L. S. (1975) *Sulfur Ylides: Emerging Synthetic Intermediates*, Vol. 31, Academic Press, New York.
43. Walsh, C. (1979) *Enzymatic Reaction Mechanisms*, W. H. Freeman and Co., New York.
44. Hsu, R. Y., Lardy, H. A., and Cleland, W. W. (1967) *J. Biol. Chem. 242*, 5315−5322.

BI034197U